Journal of Enzyme Inhibition and Medicinal Chemistry, 2010; 25(1): 13–20

informa healthcare

RESEARCH ARTICLE

Stereoselective inhibition of butyrylcholinesterase by enantiomers of *exo*- and *endo*-2-norbornyl-*N*-*n*-butylcarbamates

Shyh-Ying Chiou[1], Chun-Fu Huang[1], Shih-Jei Yeh[2], I-Ru Chen[2], and Gialih Lin[2]

[1]*Division of Neurosurgery, Chung Shan Medical University Hospital, Taichung, Taiwan, and* [2]*Department of Chemistry, National Chung-Hsing University, Taichung, Taiwan*

Abstract

Enantiomers of *exo*- and *endo*-2-norbornyl-*N*-*n*-butylcarbamates were characterized as pseudo substrate inhibitors of butyrylcholinesterase. These inhibitions discriminate enantiomers of the inhibitors and therefore show stereoselectivity for the enzyme. For inhibitions by (*R*)-(+)- and (*S*)-(–)-*exo*-2-norbornyl-*N*-*n*-butylcarbamates, *R*-enantiomer is a more potent inhibitor than *S*-enantiomer. But, for inhibitions by (*R*)-(+)- and (*S*)-(–)-*endo*-2-norbornyl-*N*-*n*-butylcarbamates, *S*-enantiomer is a more potent inhibitor than *R*-enantiomer. Optically pure (*R*)-(+)-*exo*-, (*S*)-(–)-*exo*-, (*R*)-(+)-*endo*-, and (*S*)-(–)-*endo*-2-norbornyl-*N*-*n*-butylcarbamates were synthesized from condensations of optically pure (*R*)-(+)-*exo*-, (*S*)-(–)-*exo*-, (*R*)-(+)-*endo*-, and (*S*)-(–)-*endo*-2-norborneols with *n*-butyl isocyanate, respectively. Optically pure norborneols were obtained from kinetic resolution of their racemic esters by lipase catalysis in organic solvent.

Keywords: *Butyrylcholinesterase; carbamate inhibitor; enantiomer; stereoselectivity; resolution by lipase*

Introduction

Butyrylcholinesterase (BChE, EC 3.1.1.8) is a serine hydrolase related to acetylcholinesterase (AChE, EC 3.1.1.8). Unlike AChE, which plays a vital role in the central and peripheral nervous systems, the physiological function of BChE remains unclear[1,2]. Despite having no identified endogenous substrate, BChE plays a key role in detoxification, by degrading esters such as succinylcholine and cocaine[3]. From X-ray crystallography, the active site structure of BChE is very similar to that of AChE[4,5]. Similar to AChE[6–9], the active site of BChE (Figure 1) contains (1) an esteratic site (ES) comprising the catalytic triad Ser198-His438-Glu325, which is located at the bottom of the gorge, (2) an oxyanion hole (OAH) composed of Gly116, Gly117, and Ala199, which stabilizes the tetrahedral intermediate, (3) an anionic substrate binding site (AS) composed of Trp82, where the quaternary ammonium pole of butyrylcholine (BCh) and various active site ligands binds through a preferential interaction of quaternary nitrogens with the π electrons of aromatic groups, (4) an acyl group binding site (ABS) that binds the acyl or carbamyl group of the substrate or inhibitor, and (5) a peripheral anionic binding site (PAS)[10–13] composed of Phe278, Tyr332[14], and Asp70, which is located at the entrance (mouth) of the active site gorge and may bind to tacrine-based hetero-bivalent ligands[15] and cage amines[16].

In Alzheimer's disease (AD), a neurological disorder, cholinergic deficiency in the brain has been reported[17,18]. Four drugs for the treatment of AD, tacrine (Cognex), donepezil (Aricept), rivastigmine (Exelon) (Figure 2), and galantamine (Reminyl), are dual inhibitors of AChE and BChE[18]. The additional demonstration that central BChE rather than AChE inhibition is the best correlate of cognitive improvement in AD clinical studies with the dual cholinesterase inhibitor rivastigmine (Figure 2) further suggests that BChE represents an intriguing target to develop drugs for the treatment of neurodegenerative disease[19–21]. The derivatives of physostigmine (Figure 2) are also potential drugs for

Address for Correspondence: Gialih Lin, Department of Chemistry, National Chung-Hsing University, Taichung 402, Taiwan. Tel: +886-4-2284-0411 (ext 705). Fax: +886-4-2286-2547. E-mail: gilin@dragon.nchu.edu.tw

(Received 23 October 2008; revised 12 February 2009; accepted 9 February 2009)

ISSN 1475-6366 print/ISSN 1475-6374 online © 2010 Informa UK Ltd
DOI: 10.3109/14756360902888200

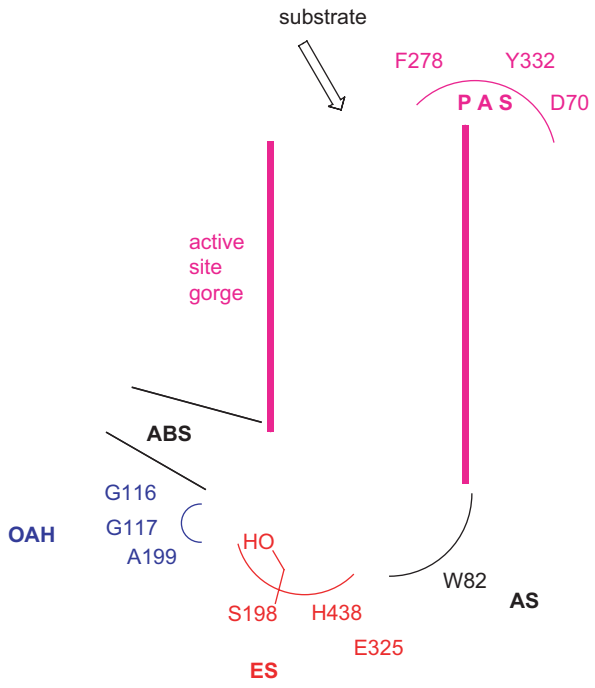

Figure 1. Active sites of human BChE[4]. The enzyme active sites consist of at least five major binding sites: (1) an oxyanion hole (OAH); (2) an esteratic site (ES) or catalytic triad; (3) an anionic substrate binding site (AS); (4) an acyl binding site (ABS); and (5) a peripheral anionic binding site (PAS).

the treatment of AD[22,23]. Since rivastigmine[24], bambuterol[25], and physostigmine are carbamates, inhibition mechanisms of both AChE and BChE by carbamates may play important roles for the treatment of AD[19–27].

Carbaryl (1-naphthyl *N*-methylcarbamate, Sevin) (Figure 2), carbofuran (Furadan), propoxur (Baygon), and aldicarb (Temik) are carbamate pesticides that have activities against a broad range of insects and low mammalian toxicity[28]. These carbamate pesticides are also dual inhibitors of AChE and BChE. Therefore, inhibition mechanisms of both AChE and BChE by carbamates may also play important roles in understanding the mechanism of pesticide toxicology. Many terpenoids are reported as inhibitors of AChE and BChE[29,30]. From these reports, AChE does not show significant stereoselectivity for enantiomers of many bicyclic monoterpenoids.

The aim of this work was to study the stereoselective inhibition of BChE by chiral norbornylcarbamates. We have reported that racemic (±)-*exo*- and (±)-*endo*-2-norbornyl-*N*-*n*-butyl-carbamates are potent pseudo substrate inhibitors of BChE[31]. In this work, we further synthesized optically pure (*R*)-(+)-*exo*-, (*S*)-(–)-*exo*-, (*R*)-(+)-*endo*-, and (*S*)-(–)-*endo*-2-norbornyl-*N*-*n*-butylcarbamates from optically pure (*R*)-(+)-*exo*-, (*S*)-(–)-*exo*-, (*R*)-(+)-*endo*-, and (*S*)-(–)-*endo*-2-norborneols. These optically pure 2-norborneols were prepared from the kinetic resolution of their racemic esters by lipase in organic solvent[32,33].

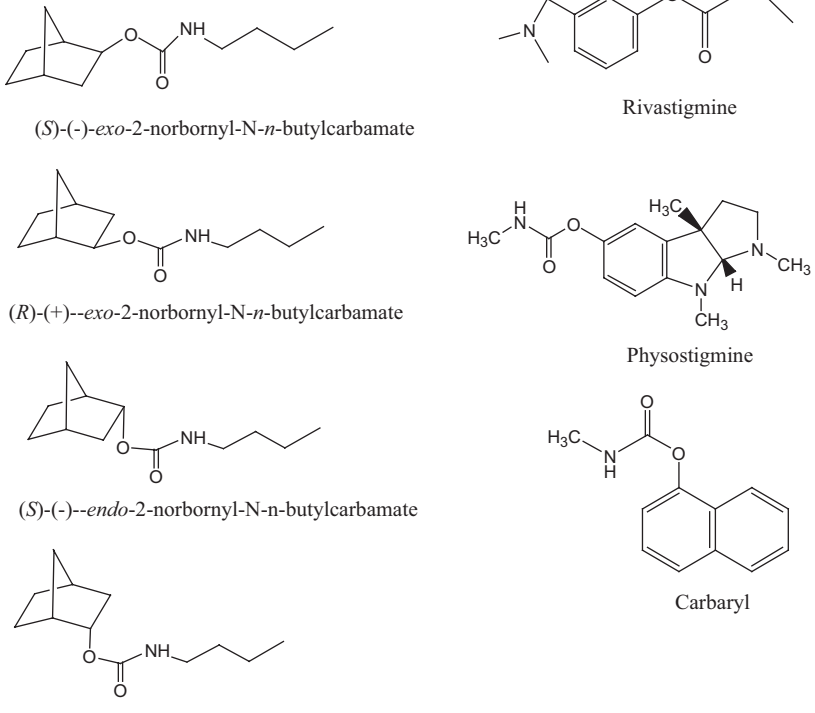

Figure 2. Structures of (*R*)-(+)-*exo*-, (*S*)-(–)-*exo*-, (*R*)-(+)-*endo*-, (*S*)-(–)-*endo*-2-norbornyl-*N*-*n*-butylcarbamates, rivastigmine, physostigmine, and carbaryl.

Materials and methods

Materials

Horse serum BChE (Sigma C7512), porcine pancreatic lipase (Sigma L3126), butyrylthiocholine chloride (BTCh), and 5,5′-dithio-bis(-2-nitrobenzoic acid) (DTNB) were obtained from Sigma (USA). (±)-*exo*- and (±)-*endo*-2-norborneol, *n*-butyl isocyanate, triethylamine, $CDCl_3$, tetramethylsilane, *t*-butyl methyl ether, butyryl chloride, pyridine, and (*S*)-(+)-α-methoxy-α-trifluoromethylphenylacetyl chloride (Mosher's acid chloride) were purchased from Aldrich (USA). Silica gel and thin layer chromatography (TLC) plate were obtained from Merck (Germany). Hexane, CH_2Cl_2, ethyl acetate, and tetrahydrofuran were obtained from Tedia (USA). Sodium dihydrogen phosphate (NaH_2PO_4:$2H_2O$), disodium hydrogen phosphate (Na_2HPO_4:$12H_2O$), hydrogen chloride (HCl), sodium hydroxide (NaOH), potassium hydroxide (KOH), calcium chloride ($CaCl_2$), and sodium chloride (NaCl) were purchased from UCW (Taiwan). Ethanol (95%) was obtained from Taiwan Tobacco & Liquid Corporation (Taiwan).

Instrumental methods

All steady state kinetic data were obtained from an ultraviolet (UV)-visible spectrophotometer (Agilent 8453) with a cell holder circulated by a water bath. ^1H, ^{13}C, and ^{19}F nuclear magnetic resonance (NMR) spectra were recorded in $CDCl_3$ at 400, 100, and 377 MHz, respectively, with internal reference tetramethylsilane (TMS) at 25°C on a Varian Gemini 400 spectrometer. Mass spectra were recorded at 71 eV in a mass spectrometer (Jeol JMS-SX/SX 102A). Elemental analyses were performed on a Heraeus instrument. Optical rotation was recorded on a polarimeter (PerkinElmer 241).

Kinetic resolution of exo- and endo-2-norborneols by lipase (Schemes 1 and 2)

(*S*)-(–)-*exo*- and (*R*)-(+)-*exo*-2-norborneol (Scheme 1)

To a *t*-butyl methyl ether (100 mL) solution of racemic (±)-*exo*-2-norbornyl butyrate (1 mmol) (synthesis from condensation of (±)-*exo*-2-norborneol with 1.2 eqs. of butyryl chloride in the presence of pyridine in CH_2Cl_2, 90–95% yield), porcine pancreatic lipase (4 g) was added. The reaction mixture was shaken at 36°C at 200 rpm for 72 h. This reaction yielded (*S*)-(–)-*exo*-2-norborneol (49% yield) (mp = 125–126°C and $[\alpha]_D^{25} = -2.70°$) ($[\alpha]_D^{25} = -3.07°$ and mp = 126–127°C from the literature[34–38]) and recovered unreactive (*R*)-*exo*-2-norbornyl butyrate (51% yield). (*R*)-(+)-*exo*-2-norborneol (mp = 125–126°C and $[\alpha]_D^{25} = +2.70°$) ($[\alpha]_D^{25} = +3.06°$ and mp = 126–127°C from the literature[34–38]) was obtained from basic hydrolysis (0.1 M KOH) of (*R*)-*exo*-norbornyl butyrate in ethanol (95%) in 99% yield.

The enantiomeric excess (e.e.) values of (*R*)-(+)-*exo*- and (*S*)-(–)-*exo*-2-norborneols from the resolutions were calculated to be 80 and 84%, respectively, from the ^{19}F-NMR spectra of their Mosher's esters, according to the following[39–41] (Figure 3 and Table 1). In an NMR tube, the condensation reaction of (*R*)-(+)-*exo*-2-norborneol (5 mM) with Mosher's chiral derivatizing agent (*S*)-(+)-α-methoxy-α-trifluoromethylphenylacetyl chloride[39] (5 mM) in $CDCl_3$ in the presence of pyridine (5 mM) was carried out at 25°C for 24 h (Scheme 3). The fluorine chemical shifts at –73.948 and –74.113 ppm with an integration ratio of 9/1 were assigned to the fluorine atoms of (2*R*)- and

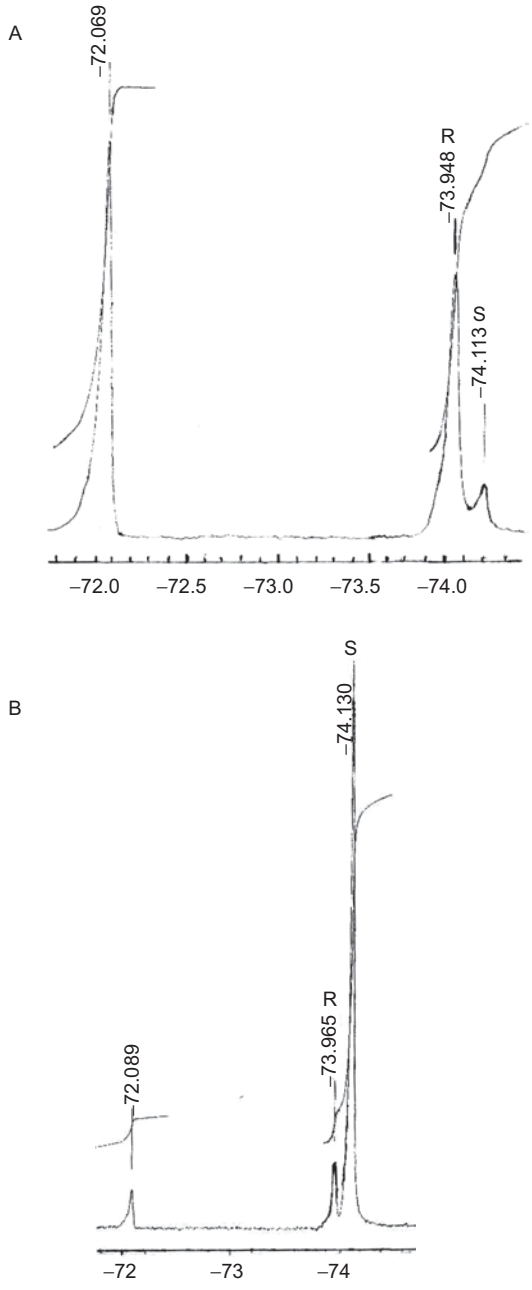

Figure 3. ^{19}F-NMR spectra after the reaction of (A) (*R*)-(–)-*exo*-2-norborneol with *S*-(+)-α-methoxy-α-trifluoromethylphenylacetyl chloride[39] in the presence of pyridine in $CDCl_3$ and (B) (*S*)-(–)-*exo*-2-norborneol with (*S*)-(+)-α-methoxy-α-trifluoromethylphenylacetyl chloride in the presence of pyridine in $CDCl_3$. For (A), –72.069–ppm was the fluorine chemical shift of unreactive (*S*)-(+)-α-methoxy-α-trifluoromethylphenylacetyl chloride. The peaks at –73.948 and –74.113 ppm were assigned to the fluorine chemical shifts of (2*R*)- and (2*S*)-*exo*-norbornyl-(*S*)-α-methoxy-α-trifluoromethylphenylacetates, respectively (Scheme 3). For (B), –72.089 ppm was the fluorine chemical shift of unreactive *S*-(+)-α-methoxy-α-trifluoromethylphenylacetyl chloride. The peaks at –73.965 and –74.130 ppm were assigned to the fluorine chemical shifts of (2*R*)- and (2*S*)-*exo*-norbornyl-(*S*)-α-methoxy-α-trifluoromethylphenylacetates, respectively (Scheme 3).

Table 1. Enantiomeric excess (%) and optical purity (%) for the kinetic resolution of racemic *exo*-2-norborneol (Scheme 1) and *endo*-2-norborneol (Scheme 2) by lipase in organic solvent.

Compound	Enantiomeric excess (%)[a]	Optical purity (%)[b]
(*R*)-(+)-*exo*-2-norborneol	80	88
(*S*)-(–)-*exo*-2-norboneol	84	90
(*R*)-(+)-*endo*-2-norborneol	90	96
(*S*)-(–)-*endo*-2-norborneol	92	96

[a]Enantiomeric excess (%) was calculated from the ratio of integration of the fluorine chemical shift of their Mosher's ester derivatives from the ^{19}F-NMR spectra (Scheme 3 and Figure 3).

[b]Optical purity (%) was calculated as $100 \times [\alpha]_D^{25}{}_{observed}/[\alpha]_D^{25}{}_{literature}$.

(2*S*)-*exo*-norbornyl-(*S*)-α-methoxy-α-trifluoromethylphenyl acetates, respectively (Scheme 3) (Figure 3A). Therefore, the enantiomeric excess of (*R*)-(+)-*exo*-2-norborneol from kinetic resolution by lipase catalysis (Scheme 1) was calculated to be 80% from integration of these two peaks (Table 1).

(*S*)-(–)-*exo*-2-norborneol (5 mM) was also condensed with Mosher's chiral derivatizing agent (*S*)-(+)-α-methoxy-α-trifluoromethylphenylacetyl chloride[39] (5 mM) in $CDCl_3$ in the presence of pyridine (5 mM) at 25°C for 24 h (Scheme 3). After reaction, the peaks at –73.965 and –74.130 ppm with an integration ratio of 92/8 were assigned to the fluorine atoms of (2*R*)- and (2*S*)-*exo*-norbornyl-(*S*)-α-methoxy-α-trifluoromethylphenyl acetates, respectively (Scheme 3) (Figure 3B). Therefore, the enantiomeric excess of (*R*)-(+)-*exo*-2-norborneol from kinetic resolution by lipase catalysis (Scheme 1) was calculated to be 84% (Table 1).

(*S*)-(–)-*endo*- and (*R*)-(+)-*endo*-2-norborneol (Scheme 2)

To a *t*-butyl methyl ether (50 mL) solution of racemic (±)-*endo*-2-norborneol (44.6 mmol) and vinyl acetate (10 mL), porcine pancreatic lipase (30 g) was added. The reaction mixture was shaken at 37°C at 200 rpm for 72 h. This reaction yielded (*R*)-(+)-*endo*-2-norbornyl acetate (49%) and recovered unreactive (S)-(–)-*endo*-norborneol (51%) (mp = 148–150°C and $[\alpha]_D^{25} = -1.81°$; mp = 151–152°C and $[\alpha]_D^{25} = -1.89°$ from the literature[34–38]). (*R*)-(+)-*endo*-2-norborneol (mp = 148–150°C and $[\alpha]_D^{25} = +1.81$; $[\alpha]_D^{25} = +1.89°$ and mp = 151–152°C from the literature[34–38]) was obtained from basic hydrolysis (0.1 M KOH) of (*R*)-*endo*-norbornyl butyrate in ethanol (95%) in 99% yield. The enantiomeric excess (e.e.) values of (*S*)-(–)-*endo*- and (*R*)-(+)-*endo*-2-norborneols from the resolutions were calculated to be 90 and 92%, respectively, from the ^{19}F-NMR spectra of their Mosher's esters (Table 1).

In an NMR tube, the condensation reaction of (*R*)-(+)-*endo*-2-norborneol (5 mM) with Mosher's chiral derivatizing agent (*S*)-(+)-α-methoxy-α-trifluoromethylphenylacetyl chloride[39] (5 mM) in $CDCl_3$ in the presence of pyridine (5 mM) was carried out at 25°C for 24 h. The fluorine chemical shifts at –73.975 and –74.152 ppm with an integration ratio of 95/5 were assigned to the fluorine atoms of (2*R*)- and (2*S*)-*endo*-norbornyl-(*S*)-α-methoxy-α-trifluoromethylphenyl acetates, respectively. Therefore, the enantiomeric excess of (*R*)-(+)-*endo*-2-norborneol from kinetic resolution by lipase catalysis (Scheme 2) was calculated to be 90% from integration of these two peaks (Table 1).

(*S*)-(–)-*endo*-2-norborneol (5 mM) was condensed with Mosher's chiral derivatizing agent (*S*)-(+)-α-methoxy-α-trifluoromethylphenylacetyl chloride[39] (5 mM) in $CDCl_3$ in the presence of pyridine (5 mM) at 25°C for 24 h. The fluorine chemical shifts at –74.026 and –74.185 ppm with an integration ratio of 96/4 were assigned to the fluorine atoms of (2*R*)- and (2*S*)-*endo*-norbornyl-(*S*)-α-methoxy-α-trifluoromethylphenyl acetates, respectively. Therefore, the enantiomeric excess of (*S*)-(–)-*endo*-2-norborneol from kinetic resolution by lipase catalysis (Scheme 2) was calculated to be 92% from integration of these two peaks (Table 1).

Synthesis of (R)-(+)-exo-, (S)-(–)-exo-, (R)-(+)-endo-, and (S)-(–)-endo-2-norbornyl-N-n-butylcarbamates

(*R*)-(+)-*exo*-, (*S*)-(–)-*exo*-, (*R*)-(+)-*endo*-, and (*S*)-(–)-*endo*-2-norbornyl-*N*-*n*-butylcarbamates were synthesized from condensation of optically pure (*R*)-(+)-*exo*-, (*S*)-(–)-*exo*-, (*R*)-(+)-*endo*-, and (*S*)-(–)-*endo*-2-norborneols, respectively, with 1.2 eqs. of *n*-butyl isocyanate in the presence of 1.2 eqs. of triethylamine in tetrahydrofuran at 25°C for 1 day (85–92% yield). All products were purified by liquid chromatography (silica gel, hexane–ethyl acetate) and were characterized by ^{1}H- and ^{13}C-NMR spectra, mass spectra, and elemental analysis as follows.

(*R*)-(+)-*exo*- and (*S*)-(–)-*exo*-2-norbornyl-*N*-*n*-butylcarbamates

^{1}H-NMR ($CDCl_3$) δ 0.92 (t, *J* = 7 Hz, 3H, carbamate ω-C*H*$_3$), 1.40 (sextet, *J* = 7 Hz, 2H, carbamate γ-C*H*$_2$), 1.0–1.6 (m, 7H, 4,5,6,7-norbornyl *H*s), 1.56 (quintet, *J* = 7 Hz, 2H, carbamate β-C*H*$_2$), 1.70 (m, 1H, norbornyl C(1)*H*), 2.24 (m, 2H, norbornyl C(3)*H*$_2$), 3.15 (t, *J* = 7 Hz, 2H, carbamate α-C*H*$_2$), 4.53 (m, 1H, norbornyl-C(2)*H*). ^{13}C-NMR ($CDCl_3$) δ 13.7 (carbamate ω-*C*H$_3$), 19.9 (carbamate β-*C*H$_2$), 24.2 (norbornyl *C*-6), 28.1 (norbornyl *C*-5), 32.1 (carbamate γ-*C*H$_2$), 35.2 (norbornyl *C*-7), 35.3 (norbornyl *C*-4), 39.6 (norbornyl *C*-3), 40.6 (norbornyl *C*-1), 41.6 (carbamate α-*C*H$_2$), 77.7 (norbornyl *C*-2), 156.4 (carbamate *C*=O). Mass spectra, exact mass: 211.157; elemental analysis: calculated for $C_{12}H_{21}NO_2$: C, 68.21; H, 10.02; N, 6.63, found C, 68.15; H, 10.32; N, 6.56%. mp 178–180°C) (decomp.).

(*R*)-(+)-*endo*- and (*S*)-(–)-endo-2-norbornyl-*N*-*n*-butylcarbamates

^{1}H-NMR ($CDCl_3$) δ 0.92 (t, *J* = 7 Hz, 3H, carbamate ω-C*H*$_3$), 1.20–1.80 (m, 11H, carbamate β- and γ-C*H*$_2$ and 4,5,6,7-norbornyl *H*s), 1.96 (m, 1H, norbornyl C(1)*H*), 2.10–2.50 (m, 2H, norbornyl C(3)*H*$_2$), 3.19 (t, *J* = 7 Hz, 2H, carbamate α-C*H*$_2$), 4.60 (br. s, 1H, carbamate NH), 4.89 (m, 1H, norbornyl-C(2)*H*). ^{13}C-NMR ($CDCl_3$) δ 13.7 (carbamate ω-*C*H$_3$), 19.8 (carbamate β-*C*H$_2$), 20.9 (norbornyl *C*-6), 29.4 (norbornyl *C*-5), 32.1 (carbamate γ-*C*H$_2$), 36.4 (norbornyl *C*-7), 36.9 (norbornyl *C*-4), 37.2 (norbornyl *C*-3), 40.4 (carbamate α-*C*H$_2$), 40.7 (norbornyl *C*-1), 75.7 (norbornyl *C*-2), 156.8 (carbamate

C=O). Mass spectra, exact mass: 211.157; elemental analysis: calculated for $C_{12}H_{21}NO_2$: C, 68.21; H, 10.02; N, 6.63, found C, 68.17; H, 10.30; N, 6.58%. mp 178–180°C (decomp.).

Data reduction

Origin (version 6.0) was used for linear and nonlinear least-squares curve fittings.

Enzyme inhibition

BChE inhibitions by the carbamate inhibitors were assayed by the Ellman method[42]. BChE-catalyzed hydrolysis of BTCh in the presence of the carbamate inhibitors and DTNB was followed continuously at 410 nm on a UV-visible spectrometer. The temperature was maintained at 25.0°C by a refrigerated circulating water bath. All inhibition reactions were performed in sodium phosphate buffer (1 mL, 0.1 M, pH 7.0) containing NaCl (0.1 M), acetonitrile (2% by volume), triton X-100 (0.5% by weight), substrate (ATCh for AChE or BTCh for BChE) (50 μM), DTNB, and varying concentrations of inhibitor. Requisite volumes of stock solution of substrate and inhibitors in acetonitrile were injected into the reaction buffer via a pipet. BChE was dissolved in sodium phosphate buffer (0.1 M, pH 7.0). The first-order rate constant (k_{app}) for inhibition was determined as described by Hosie *et al.*[43–47]. The apparent inhibition constant ($(1 + [S]/K_m)K_i$) and carbamylation constant (k_2) were obtained from the nonlinear least-squares curve fitting of the k_{app} vs. [I] plot following Equation (1) (Figure 4). Duplicate sets of data were collected for each inhibitor concentration.

$$k_{app} = k_2[I]/(K_i(1 + [S]/K_m) + [I]) \quad (1)$$

Results and discussion

Kinetic resolution of norborneols by lipase catalysis

In this article, we first report the kinetic resolution of (*R*)-(+)-*exo*-, (*S*)-(–)-*exo*-, (*R*)-(+)-*endo*-, and (*S*)-(–)-*endo*-2-norborneols by lipase catalysis in organic solvent (Schemes 1 and 2). The absolute configurations of (*S*)-(–)-*exo*-, (*R*)-(+)-*exo*-, (*S*)-(–)-*endo*-, and (*R*)-(+)-*endo*-2-norborneols were determined on the basis of their optical rotation values[34–38] and the ^{19}F-NMR spectra of their Mosher's ester derivatives[39–41] (Table 1 and Scheme 3).

Pseudo substrate inhibitions of BChE by carbamates

The mechanism for BChE-catalyzed hydrolysis of substrate is formation of the first tetrahedral intermediate via nucleophilic attack of the active site Ser (Figure 1) to substrate, then formation of the acyl enzyme intermediate from the intermediate (Scheme 4). In the presence of substrate, (*R*)-(+)-*exo*-, (*S*)-(–)-*exo*-, (*R*)-(+)-*endo*-, and (*S*)-(–)-*endo*-2-norbornyl-*N*-*n*-butylcarbamates are characterized as the pseudo or alternate[48,49] substrate inhibitors of BChE, like many other carbamates (Figure 4, Table 2, and Scheme 4)[43–47]. Presumably, the carbonyl carbons of the *n*-butylcarbamyl moieties of inhibitors are nucleophilically attacked by the active site serine of the enzyme then formation of the *n*-butylcarbamyl enzyme follows (Scheme 4).

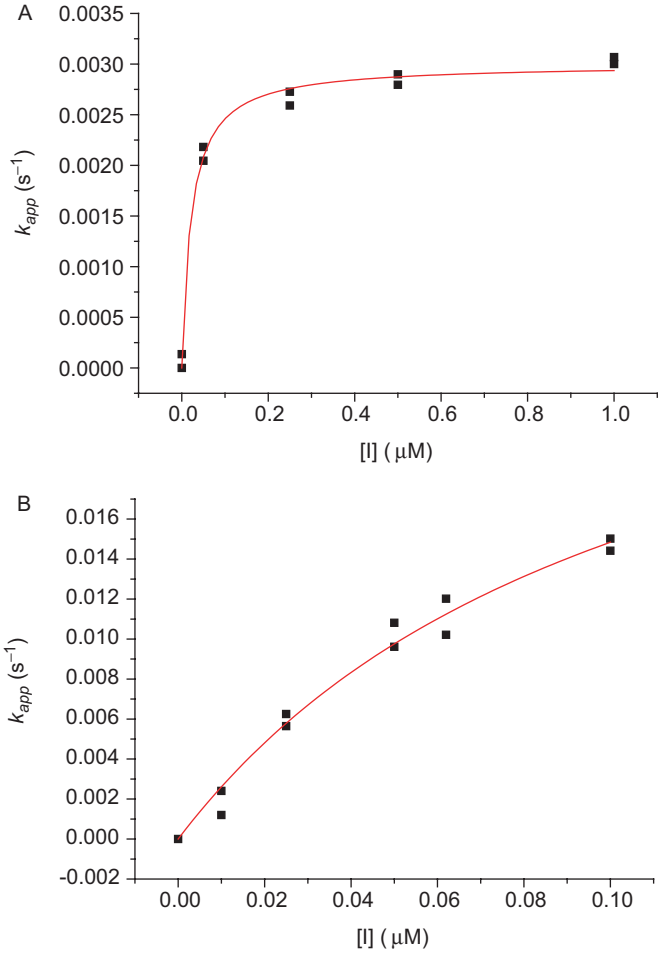

Figure 4. Nonlinear least-squares curve fittings of (A) the k_{app} vs. (*R*)-(+)-*exo*-2-norbornyl-*N*-*n*-butylcarbamate concentration ([I]) plot and (B) the k_{app} vs. (*R*)-(+)-*exo*-2-norbornyl-N-*n*-butylcarbamate concentration ([I]) plot following Equation (1) for pseudo substrate inhibition of BChE. For Figure 4A, the parameters of the fit were $k_2 = 0.0030 \pm 0.0001\ s^{-1}$ and $(1 + K_m/[S])K_i = 22 \pm 4$ nM with R= 0.9963. After calculation, $K_i = 11 \pm 2$ nM and $k_i = (270 \pm 50) \times 10^3\ M^{-1}s^{-1}$ (Table 2). For Figure 4B, the parameters of the fit were $k_2 = 0.00310 \pm 0.00007\ s^{-1}$ and $(1 + K_m/[S])K_i = 100 \pm 4$ nM with R= 0.9920. After calculation, $K_i = 50 \pm 2$ nM and $k_i = (62 \pm 3) \times 10^3\ M^{-1}s^{-1}$ (Table 2).

BChE inhibitions by (R)-(+)- and (S)-(–)-exo-2-norbornyl-N-n-butylcarbamates

Comparing the BChE inhibitory potency between both enantiomers of *exo*-2-norbornyl-*N*-*n*-butylcarbamate, *R*-enantiomer is about 3.35 times more potent than *S*-enantiomer (Table 2). Therefore, BChE shows stereoselectivity for (*R*)-(+)-*exo*-2-norbornyl-*N*-*n*-butylcarbamate over (*S*)-(–)-*exo*-2-norbornyl-*N*-*n*-butylcarbamate. K_i and k_i values for the racemic inhibitor are about the average of those of both enantiomers (Table 2). This stereopreference ($R < S$) is the same as those reported for the BChE-catalyzed hydrolysis enantiomers of

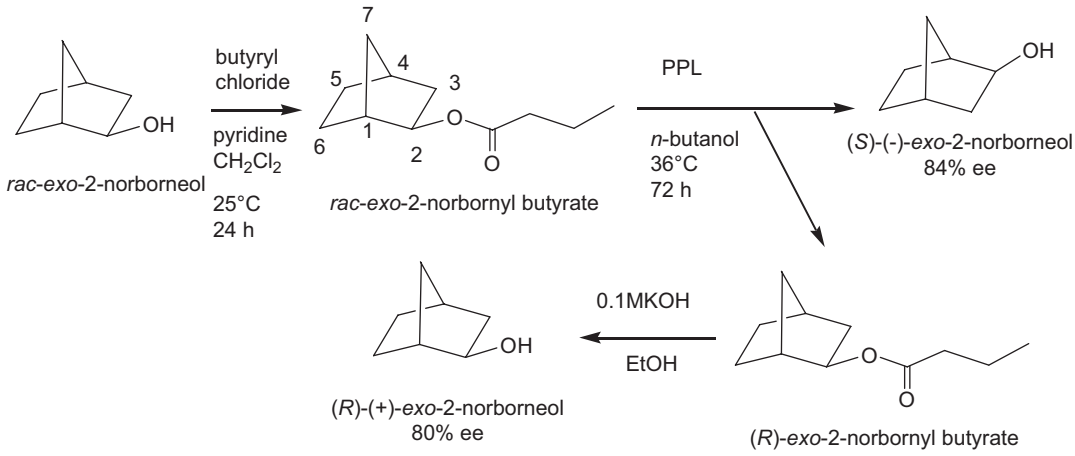

Scheme 1. Kinetic resolution of (*R*)-(+)- and (*S*)-(–)-exo-2-norborneols from lipase-catalyzed hydrolysis of racemic (±)-exo-2-norbornyl butyrate.

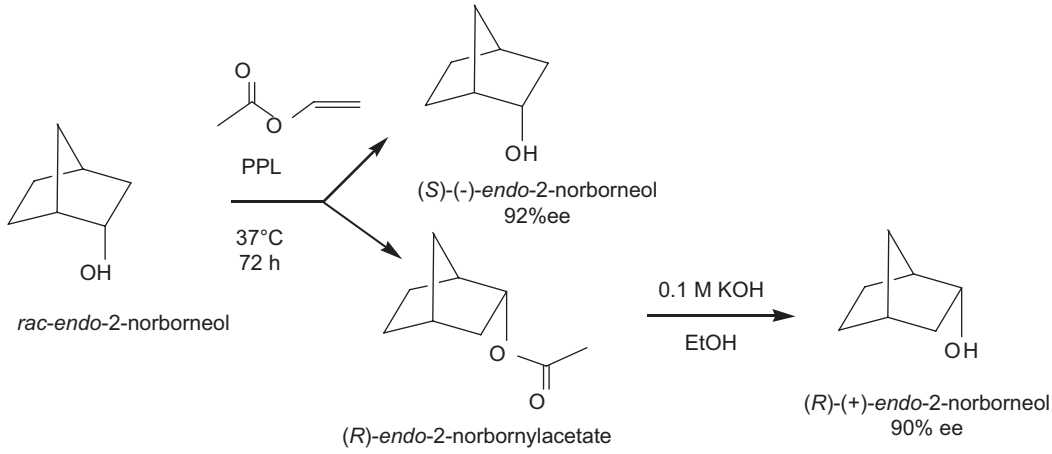

Scheme 2. Kinetic resolution of (*R*)-(+)- and (*S*)-(–)-endo-2-norborneols from lipase-catalyzed acetylation of racemic (±)-exo-2-norborneol with vinyl acetate.

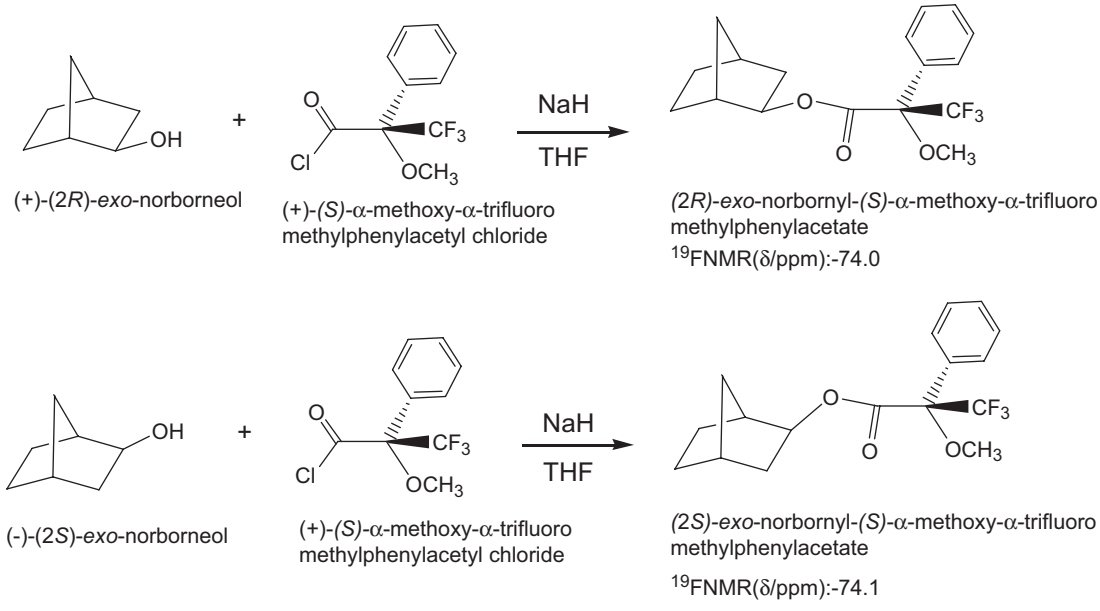

Scheme 3. Determination of enantiomeric excess and absolute configuration of (*R*)-(+)- and (*S*)-(–)-exo-2-norborneols by ^{19}F-NMR spectra of their Mosher's ester derivatives.

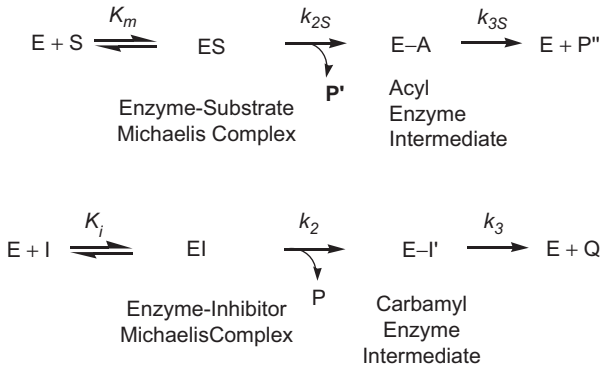

Scheme 4. Kinetic scheme for pseudo substrate inhibition of BChE by 2-norbornyl-*N*-*n*-butylcarbamate in the presence of substrate. E, enzyme; E-A, acyl enzyme; EI, enzyme–inhibitor Michaelis complex; E-I′, carbamyl enzyme; ES, enzyme–substrate Michaelis complex; I, pseudo substrate inhibitor; k_2, carbamylation constant; k_3, decarbamylation constant; k_{2S}, formation rate constant of E-A; k_{3S}, deacylation constant of E-A; K_i, inhibition constant; K_m, Michaelis–Menten constant; P, product, 2-norborneol; P′, product, thiocholine; P′′, product, butyrate; Q, product, butylcarbamic acid; S, substrate, BTCh.

Table 2. The k_2, K_i, and k_i values[a] of BChE inhibitions by stereoisomers of 2-norbornyl carbamates.

Inhibitor	K_i (nM)	k_2 (10^{-3} s^{-1})	k_i (10^3 M^{-1}s^{-1})	Enantio-selectivity[b]
(*R*)-(+)-*exo*-	11 ± 2	3.0 ± 0.1	270 ± 50	4.35
(*S*)-(-)-*exo*-	50 ± 2	3.10 ± 0.07	62 ± 3	1.00
rac-(±)-*exo*-	30 ± 8	2.9 ± 0.1	100 ± 30	1.61
(*R*)-(+)-*endo*-	5.0 ± 0.8	1.00 ± 0.05	200 ± 20	1.00
(*S*)-(-)-*endo*-	2.0 ± 0.2	1.00 ± 0.02	500 ± 50	2.50
rac-(±)-*endo*-	3.0 ± 0.6	0.98 ± 0.04	320 ± 70	1.60

[a]The apparent inhibition constant ($(1 + [S]/K_m)K_i$) and carbamylation constant (k_2) were obtained from nonlinear least-squares curve fitting of the k_{app} vs. [I] plot following Equation (1).

[b]Defined as k_i (more potent enantiomer)/k_i (less potent enantiomer).

quinuclidin-3-acetate[50], bambuterol[51], quinuclidinium benzoate[52], and cocaine[53]. Modeling both enantiomers of *exo*-2-norbornyl-*N*-*n*-butylcarbamate into the active site of BChE[4,5] (Figure 1) indicates that the norbornyl ring of (*R*)-enantiomer fits better into the AS of the enzyme than that of (*S*)-enantiomer (Figure 5A). On the other hand, an unfavorable repulsive force between the norbornyl ring of (*S*)-enantiomer and the nucleophilic serine of the enzyme has been observed in this model (Figure 5A). Therefore, BChE stereoselectively hydrolyzes *R*-enantiomers of the *exo*-substituted ring compounds such as *exo*-2-norbornyl-*N*-*n*-butylcarbamate, quinuclidin-3-acetate[50], quinuclidinium benzoate[52], and cocaine[53].

BChE inhibitions by (R)-(+)- and (S)-(–)-endo-2-norbornyl-N-n-butylcarbamates

Comparing the BChE inhibitory potency between both enantiomers of *endo*-2-norbornyl-*N*-*n*-butylcarbamate, *S*-enantiomer is 2.5 times more potent than *R*-enantiomer (Table 2). Therefore, BChE shows setereoselectivity for (*S*)-(–)-*endo*-2-norbornyl-*N*-*n*-butylcarbamate over (*R*)-(+)-*endo*-2-norbornyl-*N*-*n*-butylcarbamate. K_i and k_i values for

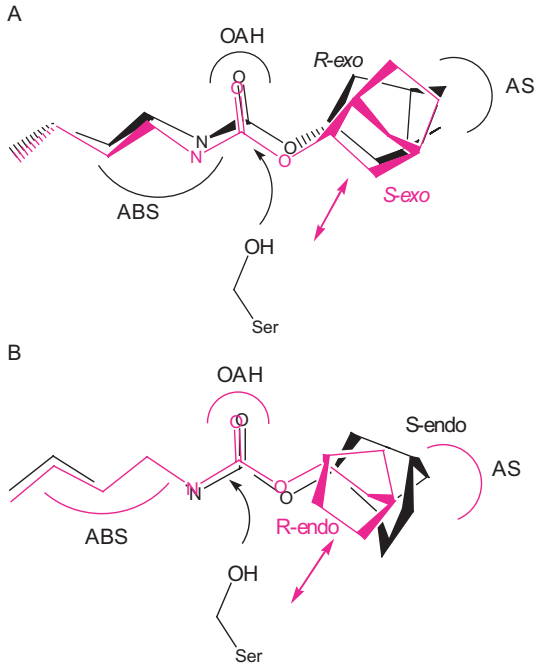

Figure 5. Superimposition of (A) (*R*)-(+)- and (*S*)-(–)-*exo*-2-norbornyl-*N*-*n*-butyl- carbamates and (B) (*R*)-(+)- and (*S*)-(–)-*endo*-2-norbornyl-*N*-*n*-butylcarbamates at their carbamyl moieties and fitting both enantiomers into the active site of BChE. For (A), an unfavorable repulsion between *S*-enantiomer and the active serine of the enzyme was observed. For (B), an unfavorable repulsion between *R*-enantiomer and the active serine of the enzyme was observed.

the racemic inhibitor are about the average of those of both enantiomers (Table 2). However, this stereopreference ($S < R$) is opposite to those reported for the BChE-catalyzed hydrolysis enantiomers of quinuclidin-3-acetate[50], bambuterol[51], quinuclidinium benzoate[52], and cocaine[53]. Modeling both enantiomers of *endo*-2-norbornyl-*N*-*n*-butylcarbamate into the active site of the X-ray structure of BChE[4,5] (Figure 1) suggests that the norbornyl ring of (*S*)-enantiomer fits better into the AS of the enzyme than (*R*)-enantiomer (Figure 5B). On the other hand, an unfavorable repulsive force between the norbornyl ring of (*R*)-enantiomer and the nucleophilic serine of the enzyme is proposed in this model (Figure 5B). The different stereopreference of BChE for *endo*-2-norbornyl-*N*-*n*-butylcarbamate may be due to the fact that the AS site of BChE strongly binds to C-7 of *endo*-2-norbornyl-*N*-*n*-butylcarbamate instead (Figure 5B).

***Declaration of interest*:** The authors report no conflicts of interest. The authors alone are responsible for the content and writing of the paper.

References

1. Massoulie J, Pezzementi L, Bon S, Krejci E, Vallette FM. *Prog Neurobiol* 1993;41:31–91.
2. Xie W-H, Stribley JA, Chatonnet A, Wilder PJ, Rizzino A, McComb RD, et al. *Pharmacol Exp Ther* 2000;293:869–902.

3. Gorelick DA. *Drug Alcohol Depend*. 1997; 48:159–165.
4. Nicolet Y, Lockridge O, Masson P, Fontecilla-Camps JC, Nachon F. *J Biol Chem* 2003; 278:41141–7.
5. Loudwig S, Nicolet Y, Masson P, Fontecilla-Camps JC, Bon S, Nachon F, et al. *ChemBioChem* 2003; 4:762–7.
6. Sussman JL, Harel M, Frolow F, Oefner C, Goldma A, Toker L, et al. *Science* 1991; 253:872–9.
7. Harel M, Sussman JL, Krejci E, Bon S, Chanal P, Massoulie J, et al. *Proc Natl Acad Sci USA* 1992; 89:10827–31.
8. Bar-On P, Millard CB, Harel M, Dvir H, Enz A, Sussman JL, et al. *Biochemistry* 2002; 41:3555–63.
9. Harel M, Quinn DM, Nair HK, Silman I, Sussman JL. *J Am Chem Soc* 1996; 118:2340–6.
10. Radic Z, Pickering NA, Vellom DC, Camp S, Taylor P. *Biochemistry* 1993; 32:12074–84.
11. Taylor P, Mayer RT, Himel CM. *Mol Pharmacol* 1994;45:74–83.
12. Pang Y-P, Quiram P, Jelacic T, Hong F, Brimjoin S. *J Biol Chem* 1996;271:23646–9.
13. Lin G, Lai C-Y, Liao W-C. *Bioorg Med Chem* 1999;7:2683–9.
14. Savini L, Gaeta A, Fattorusso C, Catalanotti B, Campiani G, Chiasserini L, et al. *J Med Chem* 2003;46:1–4.
15. Masson P, Xie W, Forment M-T, Levitsky V, Fortier P-L, Albaret C, et al. *Biochim Biophys Acta* 1999; 1433:281–93.
16. Lin G, Tsai H-J, Tsai Y-H. *Bioorg Med Chem Lett* 2003;13:2887–90.
17. Mesulam M. In: Giacobini E, ed. *Cholinesterase and Cholinesterase Inhibitors. London: Martin Dunitz,* 2000. 121–137.
18. Giacobini E. *Int J Geriatr Psychiatry* 2003;18:S1–5.
19. Greig NH, Utsuki T, Yu Q-S, Zhu X, Holloway HW, Perry T, et al. *Curr Med Res Opin* 2001; 17:1–6.
20. Mesulam MM, Guillozet A, Shaw P, Levey A, Duysen EG, Lockridge O. *Neuroscience* 2002; 110:627–39.
21. Giacobini E, Spiegel R, Enz A, Veroff AE, Cutler NR. *J Neural Transm* 2002; 109:1053–65.
22. Yu Q-S, Holloway HW, Flippen-Anderson JL, Hoffman B, Brossi A, Greig NH. *J Med Chem* 2001; 44:4062–71.
23. Stojan J, Pavlic MR. *J Enzyme Inhib* 1997;11:199–208.
24. Bartolucci C, Perola E, Cellai L, Brufani M, Lamba D. *Biochemistry* 1999;38:5714–19.
25. Kovarik Z, Simeon-Rudolf V. *J Enzyme Inhib Med Chem* 2004;19:113–17.
26. Lin G, Liu Y-C, Lin Y-F, Wu Y-G. *J Enzyme Inhib Med Chem* 2004;19:395–401.
27. Lin G, Lee Y-R, Liu Y-C, Wu Y-G. *Chem Res Toxicol* 2005;18:1124–31.
28. Baron RL. Carbamate insecticides. In: Hayes WJJ, Laws ERJ, eds. *Handbook of Pesticide Toxicology*. New York: Academic Press, 1991. 1125–1189.
29. Nisar M, Ahmad M, Wadood N, Lodhi MA, Shaheen F, Choudhary MI. *J Enzyme Inhib Med Chem* 2009; 24:47–51.
30. Miyazawa M, Yamafuji C. *J Agric Food Chem* 2005; 53:1765–8.
31. Lin G, Chen G-H, Ho H-C. *Bioorg Med Chem Lett* 1998; 8:2747–50.
32. Boland W, Frößl C, Lorenz N. *Synthesis* 1991; 12:1049–72.
33. Theil F. *Chem Rev* 1995; 95:2203–27.
34. Irwin AJ, Jones JB. *J Am Chem Soc* 1976; 98:8476–82.
35. Berson JA, Walla JS, Remanick A, Suzuki S, Reynods-Warnhoff P, Willner D. *J Am Chem Soc* 1961; 83:3986–97.
36. Nakazaki M, Chikamatsu H, Naemura K, Asao M. *J Org Chem* 1980; 45:4432–40.
37. Winstein S, Trifan D. *J Am Chem Soc* 1951; 74:1154–60.
38. Yoshizako F, Nishimura A, Chubachi M, Kirihata M. *J Ferm Bioeng* 1996; 82:601–3.
39. Dale JA, Mosher HS. *J Am Chem Soc* 1973; 95:512–19.
40. Takahashi T, Fukuishima A, Tanaka Y, Takeuchi Y, Kabuto K, Kabuto C. *Chem Commun* 2000:788–789.
41. Takahashi T, Kameda H, Kamei T, Ishizaki M. *J Fluorine Chem* 2006; 127:760–8.
42. Ellman CL, Courtney KD, Andres VJ, Featherstone RM. *Biochem Pharm* 1961; 7:88–95.
43. Hosie L, Sutton LD, Quinn DM. *J Biol Chem* 1987; 262:260–4.
44. Feaster SR, Lee K, Baker N, Hui DY, Quinn DM. *Biochemistry* 1996; 35:16723–34.
45. Feaster SR, Quinn DM. *Methods Enzymol* 1997; 286:231–52.
46. Lin G, Lai C-Y. *Tetrahedron Lett* 1995; 36:6117–20.
47. Lin G, Shieh C-T, Ho H-C, Chouhwang J-Y, Lin W-Y, Lu C-P. *Biochemistry* 1999; 38:9971–81.
48. Pietsch M, Gütschow M. *J Biol Chem* 2002; 277:24006–13.
49. Pietsch M, Gütschow M. *J Med Chem* 2005; 48:8270–88.
50. Simeon-Rudolf V, Tomic S, Bosak A, Primozic I, Orsulic M. *Chem Biol Interact* 2005; 157:420–1.
51. Bosak A, Gazic I, Vinkovic V, Kovarik Z. *Chem Biol Intact* 2008; 175:192–5.
52. Primozic I, Hrenar T, Tomic S, Meic Z. *European J Org Chem* 2003;(2):295–301.
53. Zhan C-G, Zheng F, Landry DW. *J Am Chem Soc* 2003; 125:2462–74.